6-6-2016

Tunable Split-Ring Resonators Using Germanium Telluride

C. H. Kodama
Air Force Institute of Technology

Ronald A. Coutu Jr.
Marquette University, ronald.coutu@marquette.edu

Published version. *Applied Physics Letters*, Vol. 108 (2016): 231901. DOI.
R.A. Coutu, Jr. was affiliated with the Department of Electrical and Computer Engineering, Air Force Institute of Technology, Wright-Patterson AFB, Ohio 45433, USA at the time of publication.

Tunable split-ring resonators using germanium telluride

C. H. Kodama, and R. A. Coutu

Citation: Appl. Phys. Lett. **108**, 231901 (2016); doi: 10.1063/1.4953228
View online: https://doi.org/10.1063/1.4953228
View Table of Contents: http://aip.scitation.org/toc/apl/108/23
Published by the American Institute of Physics

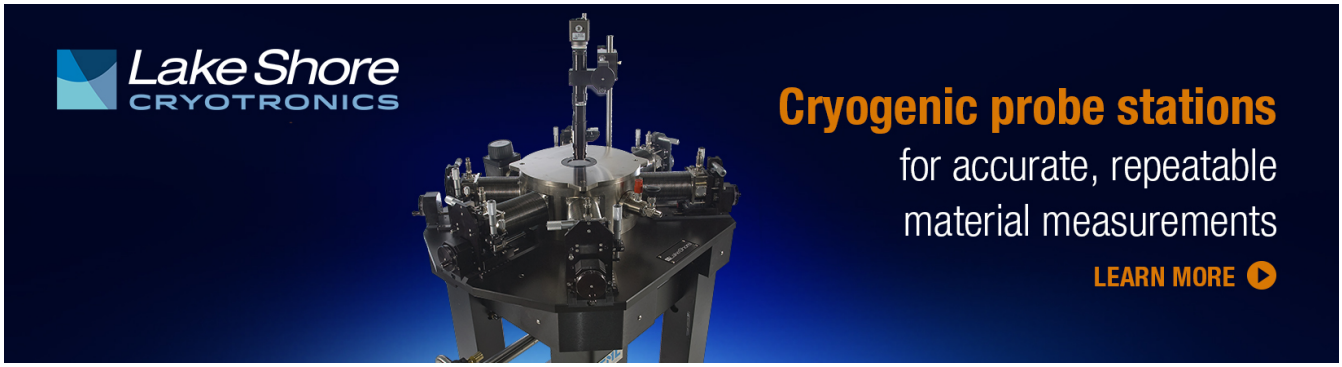

Tunable split-ring resonators using germanium telluride

C. H. Kodama and R. A. Coutu, Jr.[a)]
Department of Electrical and Computer Engineering, Air Force Institute of Technology, Wright-Patterson AFB, Ohio 45433, USA

(Received 23 March 2016; accepted 23 May 2016; published online 6 June 2016)

We demonstrate terahertz (THz) split-ring resonator (SRR) designs with incorporated germanium telluride (GeTe) thin films. GeTe is a chalcogenide that undergoes a nonvolatile phase change from the amorphous to crystalline state at approximately 200 °C, depending on the film thickness and stoichiometry. The phase change also causes a drop in the material's resistivity by six orders of magnitude. In this study, two GeTe-incorporated SRR designs were investigated. The first was an SRR made entirely out of GeTe and the second was a gold SRR structure with a GeTe film incorporated into the gap region of the split ring. These devices were characterized using THz time-domain spectroscopy and were heated *in-situ* to determine the change in the design operation with varying temperatures.

[http://dx.doi.org/10.1063/1.4953228]

Terahertz (THz) technology is an emerging field which has many applications in areas such as biomedical spectroscopy,[1] security screening,[2] and communications.[3] The THz spectrum, defined as frequencies between 300 GHz and 10 THz, has frequently been called the THz "gap" because of a lack of easy methods to generate, detect, and modulate THz waves.[1] However, there has been recent progress in methods for better control THz waves, using technology such as photonic crystals, quantum cascade lasers, high-speed rectifying diodes, and metamaterials.[4] The utilization of metamaterials is an interesting and promising approach, especially because subwavelength periodic structures needed to make metamaterials for THz wavelengths of ~100 μm can easily be made with integrated circuit (IC) and microelectromechanical systems (MEMS) fabrication technologies. These methods can create devices with minimum feature sizes on the order of 1 μm. Several actively tunable metamaterial designs have been demonstrated in the literature, using MEMS,[5–9] photoconductive silicon,[10] high mobility electron transistors (HEMTs),[11] and Schottky diodes.[12,13]

In this study, we investigate incorporating germanium telluride (GeTe) in metamaterial elements in order to create a tunable response. GeTe is a chalcogenide phase-change material with a six order of magnitude difference in resistivity between its crystalline and amorphous states.[14] The phase change occurs at the GeTe crystallization temperature (T_c) of approximately 180–230 °C, with the exact temperature being dependent on the underlying substrate material, the film thickness (as shown in Figure 1), or the stoichiometry[15,16] of the deposited GeTe film. Crystalline GeTe (c-GeTe) has a rhombohedral, distorted rocksalt crystal structure, with approximately 10% vacancies in the germanium sub-lattice causing p-type conductivity in the material.[17–19] Whereas simple heating can be used to crystallize amorphous GeTe (a-GeTe), c-GeTe can be transitioned back into a-GeTe using short electrical or optical pulses.[20,21] There is much current research interest in using chalcogenides like GeTe for applications such as phase change random access memory (PCRAM)[22] and high-speed switching.[21]

For the fabrication of the devices in this study, a Denton Discovery 18 sputtering system was used to RF sputter GeTe using a 99.999% pure, 50/50 GeTe target. The sputtering chamber was set to a pressure of 10 mTorr with a 20.1 sccm flow of argon. The thickness of all deposited GeTe layers was 300 nm. Devices with gold had the metal evaporated using a Torr International electron beam evaporator to a thickness of 280 nm, with an additional 20 nm titanium adhesion layer underneath it. All deposited layers were patterned using a bi-layer liftoff process utilizing SF-11 and S1805 photoresists. The devices were fabricated on a 1 mm-thick, intrinsic silicon substrate.

All fabricated devices were measured in a TeraView THz time-domain spectroscopy (THz-TDS) system with a

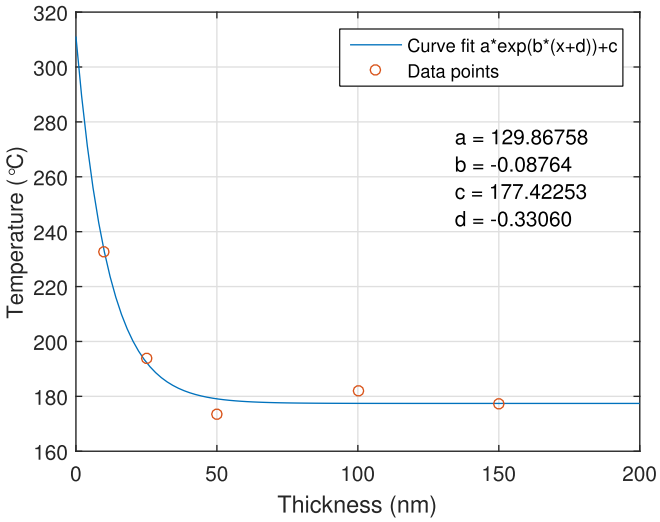

FIG. 1. Variation of crystallization temperature vs film thickness for germanium telluride on an intrinsic silicon substrate, shown with an exponential curve fit.

[a)]Author to whom correspondence should be addressed. Electronic mail: ronald.coutu@afit.edu

variable temperature cell. In THz-TDS, picosecond pulses of THz radiation were transmitted through a material under test and measured in order to characterize the material. A fast Fourier transform (FFT) was applied to the measured THz pulse data to view the pulse in the frequency domain, and these data were divided by the FFT data from a reference pulse to view the frequency-dependent transmission response of the sample material. Each measurement consisted of 5000 sequential scans of the sample material taken at a rate of 30 scans per second. For the GeTe-incorporated structures, temperature-dependent data were taken from 30 °C to 250 °C using a temperature controller with a ramp rate of 10 °C/min. Measurements were spaced by five additional minutes to ensure temperature uniformity in the measurement cell. Measurements were taken at incremental steps at 30, 100, 150, 180, 190, 200, 210, 220, and 250 °C. After heating to 250 °C, the samples were measured with decreasing temperature in steps at 200, 150, 100, 50, and 30 °C. A final measurement of the sample, labeled "R.T.," was taken 24 h after the heating experiment.

The metamaterial unit cell used in this research was the split-ring resonator (SRR) structure. An array of these SRRs (without GeTe incorporation) is shown in Figure 2(a). The SRRs shown in the figure have a 5 μm line width, 20 μm square side length, 3 μm gap width, and a 39 μm periodicity between elements. Figure 2(b) shows the measured transmission response of this SRR array and compares it to simulated results. A sample's transmission response is defined as

$$T(f) = \frac{E_t}{E_r}, \tag{1}$$

where E_t is the electric field spectrum of a measured sample and E_r is the electric field spectrum of a reference sample, which in this case consists of a measurement of a piece of bare substrate. In all measurements, the incident THz waves were polarized such that the electric field aligned with the gap, as shown in Figure 2(a). The symmetry of the SRR and its periodic arrangement dictates that the overall metamaterial will have a biaxial response with an additional bianisotropic coupling term between electric fields in the x-direction and magnetic fields in the z-direction (axis orientations are shown in Figure 2(a)).[23–25] Thus, the transmission response shown in Fig. 2(b) can be attributed to the ε_{xx} and ζ_{zx} components of the metamaterial's $\overleftrightarrow{\varepsilon}$ and $\overleftrightarrow{\zeta}$ tensors, respectively.

The simulated data were found using CST MICROWAVE STUDIO®. Simulations were performed using unit cell (Floquet) boundary conditions, with waveguide ports at normal incidence to the metamaterial. The waveguide ports supported the first two Floquet modes of the model. In the simulations, the SRRs were modeled with a frequency-independent conductivity of 45.2 S/μm and had a simulated silicon substrate with a dielectric constant of 12.04. A constant conductivity model can be used instead of the more complete Drude model for gold since the relaxation time, τ, of the metal is on the order of 10^{-14} s.[26] Although gold is known to have decreasing conductivity at or near its percolation transition,[27,28] the 300 nm gold films in this study were thick enough to ensure conductivities comparable to the bulk material value of 45.2 S/μm. In the complex dielectric constant, the constant conductivity model manifests itself as a significant contributing factor in the imaginary ε_2 term as

$$\tilde{\varepsilon} = \varepsilon_1 - j\varepsilon_2 = \varepsilon_1 - \frac{\sigma}{\varepsilon_0 \omega}, \tag{2}$$

where ε_1 is the real component of the dielectric constant (due to bound electrons[26]), σ is the constant conductivity, ω is the angular frequency, and ε_0 is the free space permittivity constant. In the THz region for gold, the $\sigma/(\varepsilon_0\omega)$ term has a magnitude on the order of 10^6, which makes the much smaller ε_1 term negligible. In simulation, ε_1 was set to 1 and was not expected to impact simulation results.

The silicon dielectric constant was characterized using a fixed-point algorithm on measured THz-TDS transmission data of a silicon sample.[29]

The transmission curves shown in Figure 2(b) have two main notch points, one at approximately 0.8 THz and the other at 2.2 THz. The 0.8 THz resonance is the quasi-static LC resonance[30] which can be shifted laterally by varying the loop inductance or split gap capacitance of the SRR. The LC resonance can also be viewed as a 1st order plasmon resonance of the structure.[31] At plasmon resonances, the SRR perimeter approximately matches an integer multiple of the plasmon half-wavelength.[32] Only the LC resonance, and higher order resonances with odd half-wavelength multiples, were observed in the transmission response due to the symmetry mismatch between the SRR orientation and the incident electric field polarization.[31] The 2.2 THz notch seen in the transmission response is the third order plasmon resonance. There were other high-frequency notches seen in the

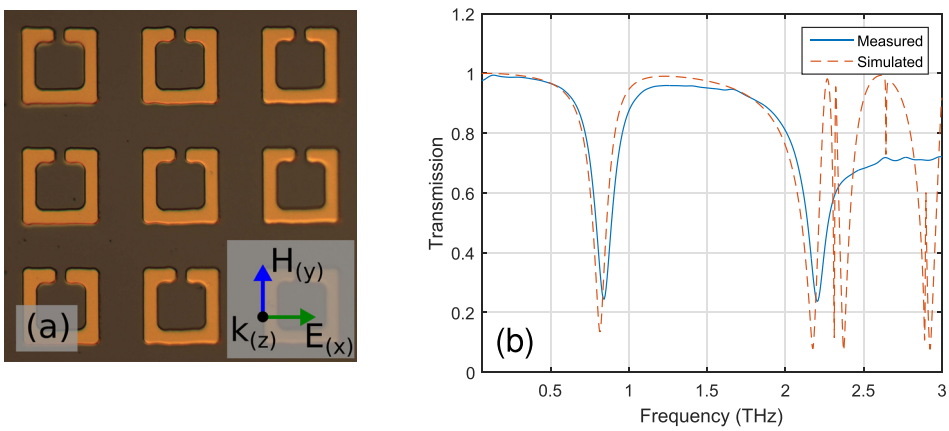

FIG. 2. Gold split-ring resonators (SRRs) are shown in (a), with axis labels showing the orientation of the incident wave. The label subscripts in parentheses specify the x, y, and z axes. The measured and simulated response of the gold SRRs are shown in (b).

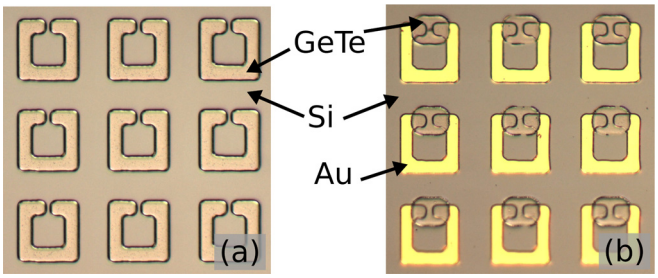

FIG. 3. Split ring resonators (SRRs) made out of germanium telluride (GeTe) are shown in (a). SRRs made of gold with additional GeTe films in the gaps of the split rings are shown in (b). The GeTe layer, gold (Au) layer, and the intrinsic silicon (Si) substrate are also labeled.

simulation, but these did not resolve well in the measurements. This was most likely due to the THz-TDS pulses having lower spectral power at the higher frequencies.

The two GeTe-incorporated SRR designs are shown in Figure 3. The "GeTe SRR" design shown in Figure 3(a) is simply an SRR array made completely out of GeTe. In the second "GeTe-in-gap SRR" design, shown in Figure 3(b), the SRRs are made out of gold, with a layer of GeTe between the splits of each SRR. Both SRR designs have the same basic geometry as the SRRs shown in Figure 2(a). The additional GeTe rectangles in the GeTe-in-gaps design are approximately 14 μm by 10 μm.

The temperature-dependent THz responses of the GeTe SRR and GeTe-in-gap SRR designs are shown in Figures 4 and 5, respectively. Starting with the 190 °C measurement, both SRR designs transitioned (i.e., crystallized) and displayed metallic behavior. This was evident by the sudden change in the transmission curve between the measurements taken at 180 and 190 °C. The GeTe SRRs exhibited an overall decrease in transmission amplitude, and the GeTe-in-gap SRRs displayed a significant change in the transmission shape. These altered transmission responses persisted after the sample was subsequently cooled due to the nonvolatile (latching) behavior of the GeTe transition.

During the heating measurements, further heating past the crystallization temperature resulted in a decrease in transmission, seemingly indicating that the sample was becoming more conductive at higher temperatures. However, GeTe is known to become less conductive at higher temperatures.[33] The slow rise in conductivity, as a function of temperature, is therefore attributed to increase numbers of thermal induced free carriers in the silicon substrate.[34]

There is a noticeable difference between the last *in-situ* measurement taken at 30 °C and the subsequent room temperature (R.T.) measurement, which were expected to be identical. This observation supports the claim of an increased number of carriers generated during thermal testing. Additionally, the mismatch can be attributed to gradual changes in the transmitted THz pulse shape and strength over the course of the temperature measurement, which can take an upwards of 6 h. For the measurement of thin films with THz-TDS, the sample measurement should be taken immediately after the reference measurement in order to minimize the effects of these gradual changes.[35] However, since the sample is measured in a heated, evacuated chamber, the reference cannot be re-measured in between each *in-situ* temperature measurement. For the R.T. transmission curve, however, the reference measurement was taken immediately before the sample measurement, which resulted in a more accurate result for the final characterization of the SRRs with c-GeTe.

The initial a-GeTe and final c-GeTe measurements of both SRR designs were compared with computer simulations

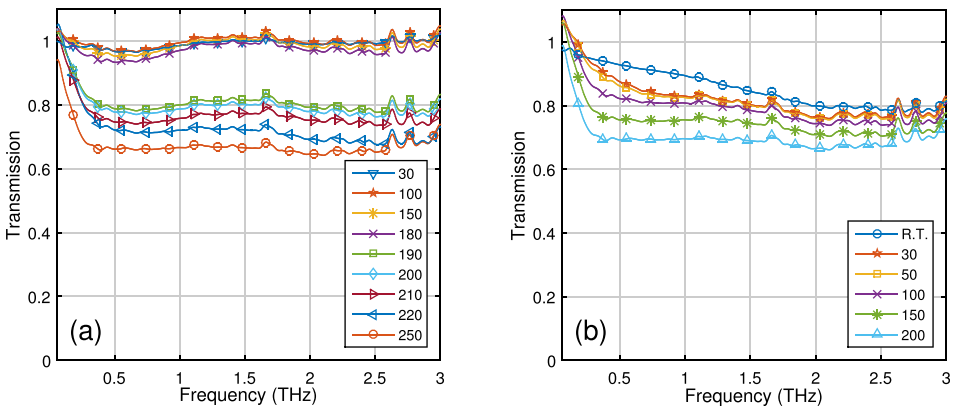

FIG. 4. Transmission response of germanium telluride split-ring resonators with (a) increased and (b) subsequently decreased temperature.

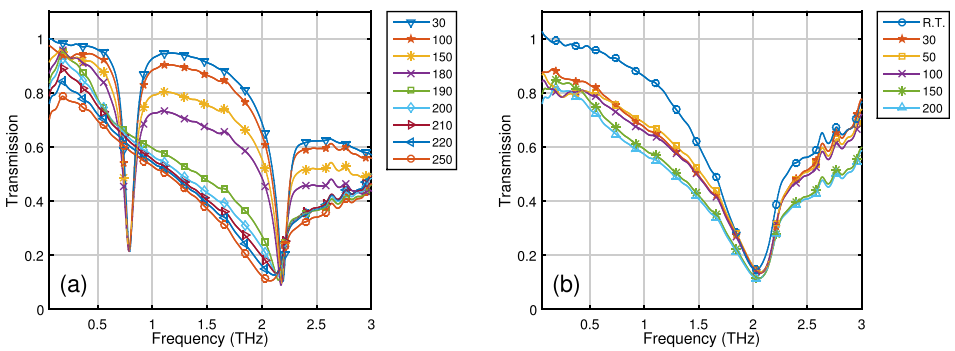

FIG. 5. Transmission response of germanium telluride in gap split-ring resonators with (a) increased and (b) subsequently decreased temperature.

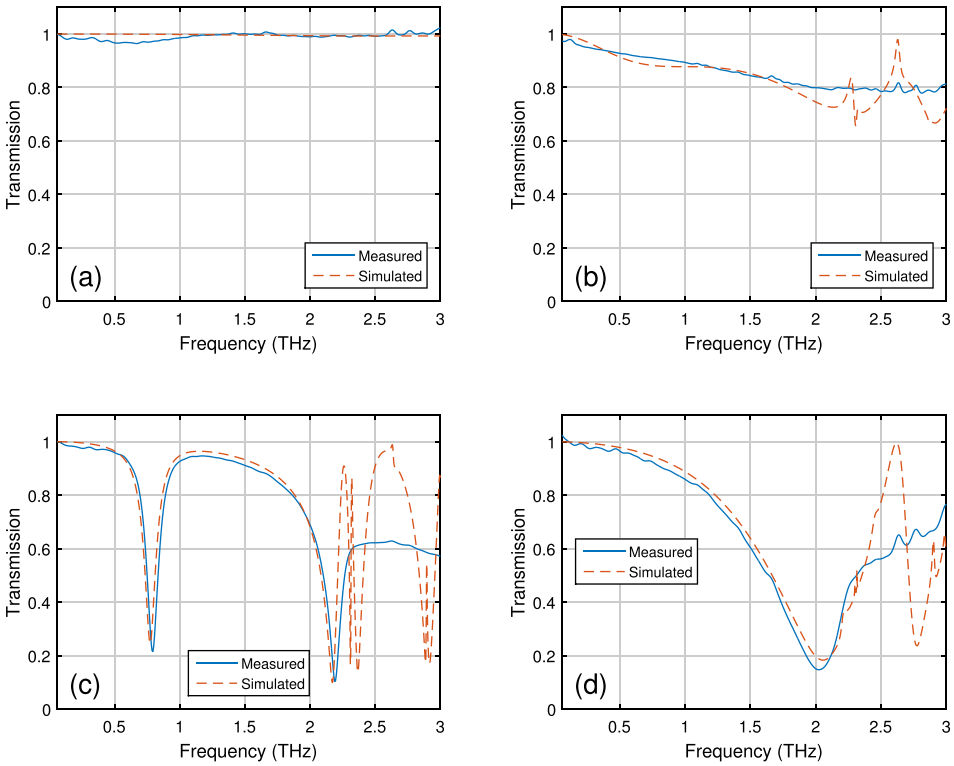

FIG. 6. Simulated and measured comparison for (a) amorphous germanium telluride (a-GeTe) split-ring resonator (SRR), (b) crystalline GeTe (c-GeTe) SRR, (c) a-GeTe-in-gaps SRR, and (d) c-GeTe-in-gaps SRR.

of the structures using CST MICROWAVE STUDIO®. The frequency-dependent THz conductivities and permittivities of GeTe in the amorphous and crystalline states are available in the literature[36,37] and were used for these simulations. The measured and simulated results are shown in Figure 6.

After heating past the crystallization temperature, sharp resonances were expected to appear in the THz transmission response of the GeTe SRRs. Although the overall transmission through the SRRs decreased, the magnitude of the decrease was very slight, and there were no sharp resonances in the response. This is likely due to ohmic losses in the c-GeTe. Although c-GeTe is known to be conductive, it is not an ideal conductor, like gold, for conducting at THz speeds. These ohmic losses in c-GeTe were high enough to cause an over-damped situation in the SRR current oscillations that normally occur at resonance. For the c-GeTe SRR, this resulted in the complete absence of the 0.8 THz resonance and a marked attenuation in the 2.2 THz resonance.

The transmission response of the GeTe-in-gap SRRs changed drastically after crystallization. The LC resonance at 0.8 THz, present in the a-GeTe state, was completely eliminated upon transition to c-GeTe. The higher order resonance remained, although it was shifted and had a wider bandwidth. Unlike the GeTe SRRs, the GeTe-in-gap SRRs were not strongly affected by the ohmic losses in c-GeTe. Since they only had a relatively small amount of GeTe in the gap section of the otherwise completely metallic (i.e., gold) SRRs, the GeTe-in-gap SRRs only had a small fraction of the ohmic loss when compared to SRRs made completely from GeTe.

The absence of the LC resonance after heating of the GeTe-in-gap SRRs can be attributed to the GeTe rectangles creating conducting paths across the SRR gaps, effectively shorting out the capacitance necessary for the LC resonance. From the perspective of plasmon resonances, the conducting path created by the GeTe rectangles effectively adds a degree of reflection symmetry to the SRR, which in turn restricts the SRR from having plasmon resonances with an odd number of nodes, including the LC resonance.[31] This also indicates that the shift seen in the higher frequency notch is really a switch from the third order to the second order plasmon resonance. This resonance has a higher bandwidth because the second order mode is essentially a dipolar resonance, giving it a stronger tendency to radiate.

As the GeTe-in-gap SRR clearly demonstrates, there is much potential for GeTe to provide significant tunability of metamaterial devices. A GeTe-incorporated metamaterial can be utilized, for example, as a thermal sensor or fuse where the fusing temperature is tuned by changing either the GeTe film thickness (illustrated in Figure 1) or its stoichiometry.[15,16] Temperatures exceeding the threshold are readily detected due to the drastic blueshift in the metamaterial's transmission response at the transition temperature (shown in Figures 5 and 6). By adding an additional circuit for electrical GeTe switching or by optimizing the GeTe film parameters for optical switching, GeTe-incorporated metamaterials can also have applications in modulation. For example, the absence or presence of the LC resonance in the GeTe-in-gaps SRR could be used for a frequency-selective amplitude modulation scheme, or the shift between different plasmon modes could be used for frequency modulation.

This research was supported by the Air Force Office of Scientific Research (AFOSR Grant No. F4FGA05069J001). The authors thank Alex Gwin and Jimmy Lohrman for assisting with data collection and the Air Force Institute of Technology (AFIT) cleanroom technician, Mr. Rich Johnston, for assistance with processing.

The views expressed in this paper are those of the authors and do not reflect the official policy or position of the U.S. Air Force, Department of Defense, or the U.S. government.

[1]R. A. Cheville, in *Terahertz Spectroscopy: Principles and Applications*, 1st ed., edited by S. L. Dexheimer (CRC Press, 2007), p. 39.
[2]J. F. Federici, B. Schulkin, F. Huang, D. Gary, R. Barat, F. Oliveira, and D. Zimdars, Semicond. Sci. Technol. **20**, S266 (2005).
[3]J. F. Federici, L. Moeller, and K. Su, in *Handbook of Terahertz Technology for Imaging, Sensing and Communications*, edited by D. Saeedkia (Woodhead Publishing, 2013), pp. 156–214.
[4]B. Erik, H. Heinz-Wilhelm, and M. F. Kimmitt, *Terahertz Techniques* (Springer, 2012).
[5]H. Tao, A. C. Strikwerda, K. Fan, W. J. Padilla, X. Zhang, and R. D. Averitt, J. Infrared, Millimeter, Terahertz Waves **32**, 580 (2011).
[6]F. Ma, L. Yu-Sheng, Z. Xinhai, and C. Lee, Light Sci. Appl. **3**, e171 (2014).
[7]H. Tao, A. Strikwerda, C. Bingham, W. J. Padilla, X. Zhang, and R. D. Averitt, *Progress in Electromagnetics Research Symposium* (Electromagnetics Academy, 2008), pp. 856–859.
[8]R. A. Coutu, Jr., P. J. Collins, E. A. Moore, D. Langley, M. E. Jussaume, and L. A. Starman, Microelectromech. Syst. J. **20**, 1366 (2011).
[9]E. A. Moore, D. Langley, M. E. Jussaume, L. A. Rederus, C. A. Lundell, R. A. Coutu, Jr., P. J. Collins, and L. A. Starman, Exp. Mech. **52**, 395–403 (2012).
[10]H.-T. Chen, J. F. O'Hara, A. K. Azad, A. J. Taylor, R. D. Averitt, D. B. Shrekenhamer, and W. J. Padilla, Nat. Photonics **2**, 295 (2008).
[11]D. Shrekenhamer, S. Rout, A. C. Strikwerda, C. Bingham, R. D. Averitt, S. Sonkusale, and W. J. Padilla, Opt. Express **19**, 9968 (2011).
[12]K. Fan and W. J. Padilla, Mater. Today **18**, 39 (2015).
[13]H.-T. Chen, W. J. Padilla, J. M. O. Zide, A. C. Gossard, A. J. Taylor, and R. D. Averitt, Nature **444**, 597 (2006).
[14]A. H. Gwin, C. H. Kodama, T. V. Laurvick, R. A. Coutu, and P. F. Taday, Appl. Phys. Lett. **107**, 031904 (2015).
[15]N. Yamada, in *Phase Change Materials: Science and Applications*, 1st ed., edited by S. Raoux and M. Wuttig (Springer, New York, NY, 2009), pp. 199–226.
[16]N. Pashkov, G. Navarro, J.-C. Bastien, M. Suri, L. Perniola, V. Sousa, S. Maitrejean, A. Persico, A. Roule, A. Toffoli, G. Reimbold, B. De Salvo, O. Faynot, P. Zuliani, and R. Annunziata, in *2011 Proceedings of the European Solid-State Device Research Conference* (IEEE, 2011), pp. 91–94.
[17]A. V. Kolobov, J. Tominaga, P. Fons, and T. Uruga, Appl. Phys. Lett. **82**, 382 (2003).
[18]A. H. Edwards, A. C. Pineda, P. A. Schultz, M. G. Martin, A. P. Thompson, and H. P. Hjalmarson, J. Phys.: Condens. Matter **17**, L329 (2005).
[19]P. Fons, in *Phase Change Materials: Science and Applications*, 1st ed., edited by S. Raoux and M. Wuttig (Springer, New York, NY, 2009), pp. 149–174.
[20]X. Sun, E. Thelander, P. Lorenz, J. W. Gerlach, U. Decker, and B. Rauschenbach, J. Appl. Phys. **116**, 133501 (2014).
[21]N. El-Hinnawy, P. Borodulin, B. P. Wagner, M. R. King, E. B. Jones, R. S. Howell, M. J. Lee, and R. M. Young, Appl. Phys. Lett. **105**, 013501 (2014).
[22]L. van Pieterson, in *Phase Change Materials: Science and Applications*, 1st ed., edited by S. Raoux and M. Wuttig (Springer, New York, NY, 2009), pp. 81–98.
[23]V. Dmitriev, Prog. Electromagn. Res. **28**, 43 (2000).
[24]V. Dmitriev, in *Theory and Phenomena of Metamaterials*, edited by F. Capolino (CRC Press, 2009).
[25]W. J. Padilla, Opt. Express **15**, 1639 (2007).
[26]Y. S. Lee, *Principles of Terahertz Science and Technology* (Springer US, 2009).
[27]M. Walther, D. G. Cooke, C. Sherstan, M. Hajar, M. R. Freeman, and F. A. Hegmann, Phys. Rev. B **76**, 125408 (2007).
[28]N. Laman and D. Grischkowsky, Appl. Phys. Lett. **93**, 051105 (2008).
[29]W. Withayachumnankul, B. Ferguson, T. Rainsford, S. P. Mickan, and D. Abbott, in *Microtechnologies for the New Millennium 2005* (2005), pp. 221–231.
[30]W. Withayachumnankul and D. Abbott, IEEE Photonics J. **1**, 99 (2009).
[31]C. Rockstuhl, F. Lederer, C. Etrich, T. Zentgraf, J. Kuhl, and H. Giessen, Opt. Express **14**, 8827 (2006).
[32]R. Marqués, F. Martín, and M. Sorolla, *Metamaterials with Negative Parameters: Theory, Design and Microwave Applications*, 1st ed. (Wiley, Hoboken, 2013).
[33]S. K. Bahl and K. L. Chopra, J. Appl. Phys. **41**, 2196 (1970).
[34]R. S. Muller, T. I. Kamins, and M. Chan, *Device Electronics for Integrated Circuits*, 3rd ed. (Wiley, New York, NY, 2003).
[35]W. Withayachumnankul, J. F. O'Hara, W. Cao, I. Al-Naib, and W. Zhang, Opt. Express **22**, 972 (2014).
[36]F. Kadlec, C. Kadlec, and P. Kužel, Solid State Commun. **152**, 852 (2012).
[37]F. Kadlec, C. Kadlec, P. Kuzel, and J. Petzelt, Phys. Rev. B **84**, 205209 (2011).